

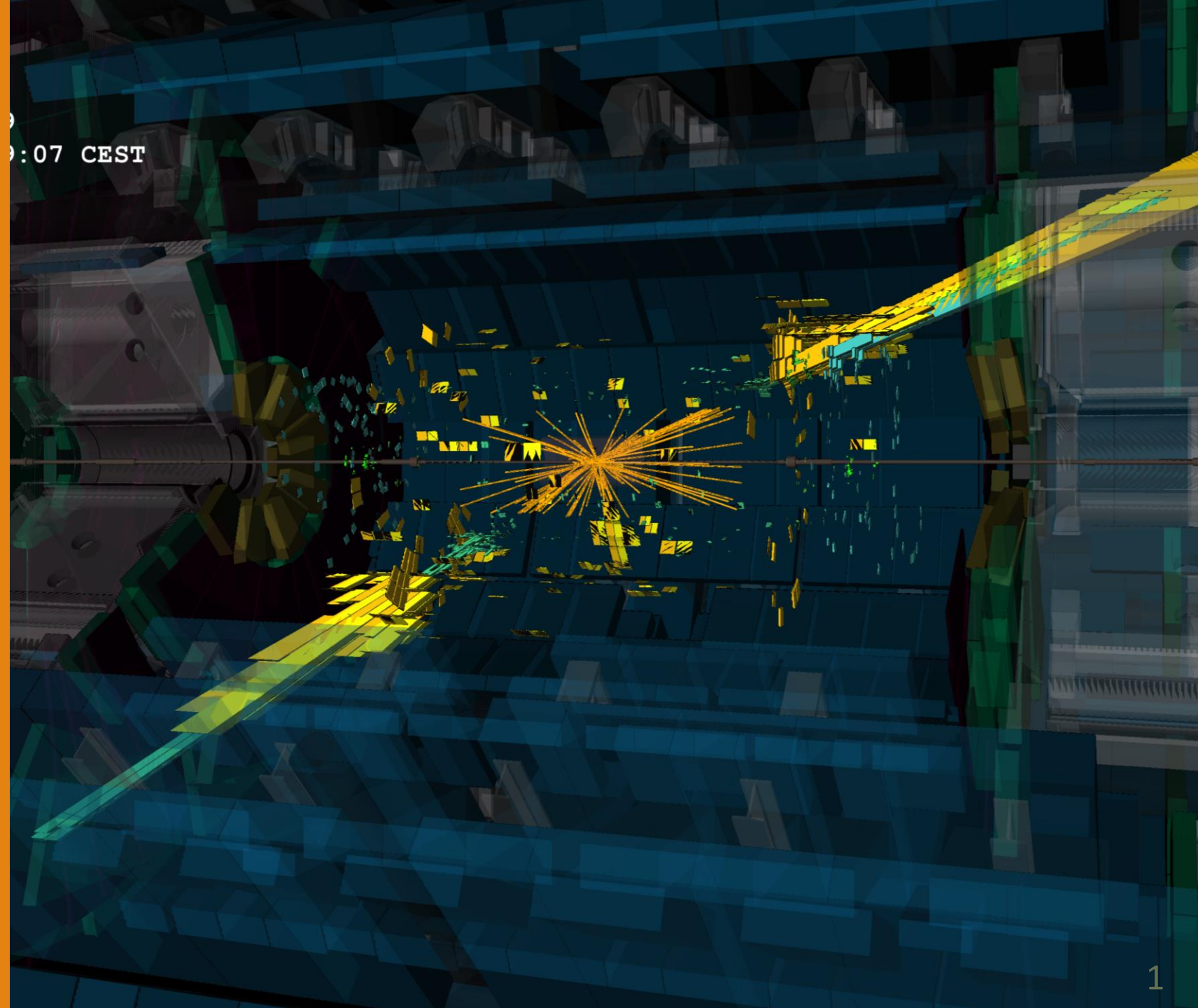
# Redefining Performance: New Techniques for ATLAS Jet Calibration

Louis Ginabat

LPNHE/CNRS  
On behalf of the ATLAS  
Collaboration

HEP2023

January 12<sup>th</sup>, 2023



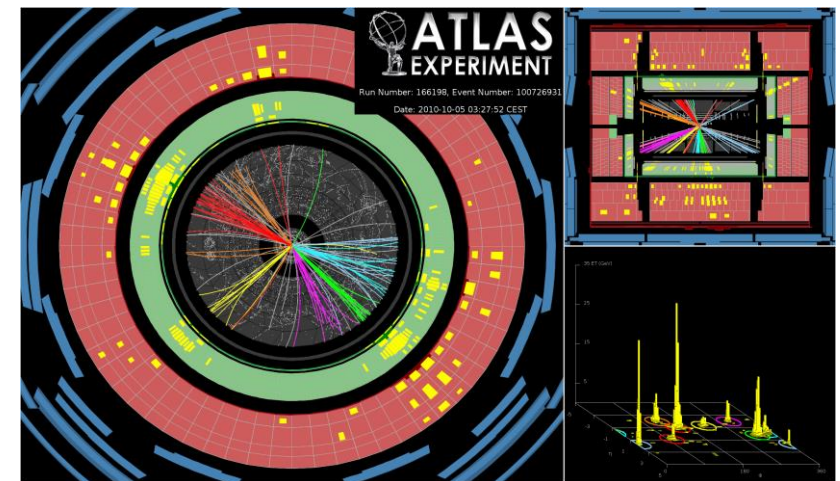
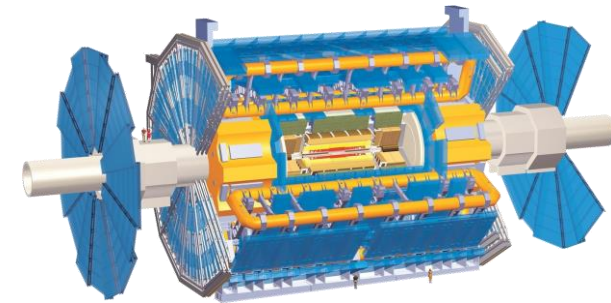
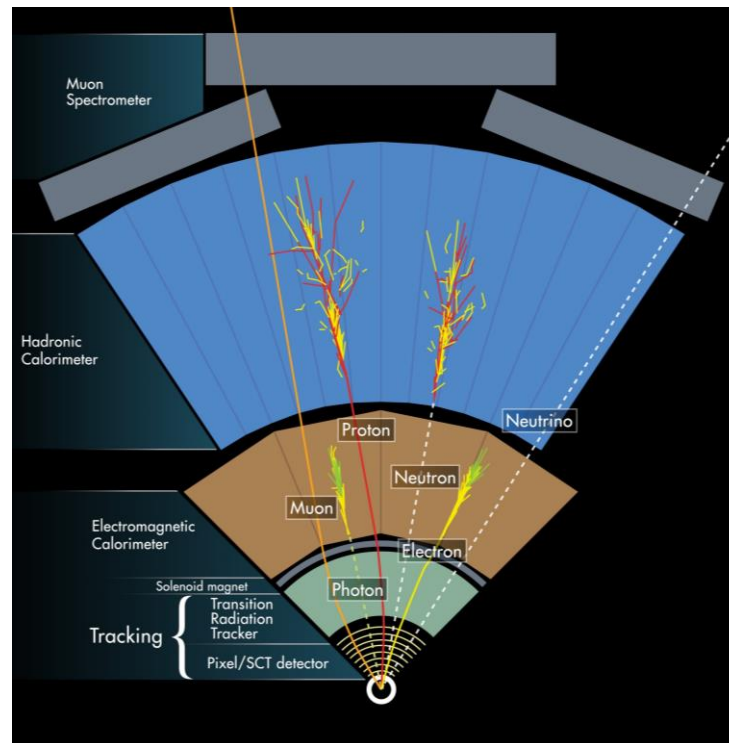
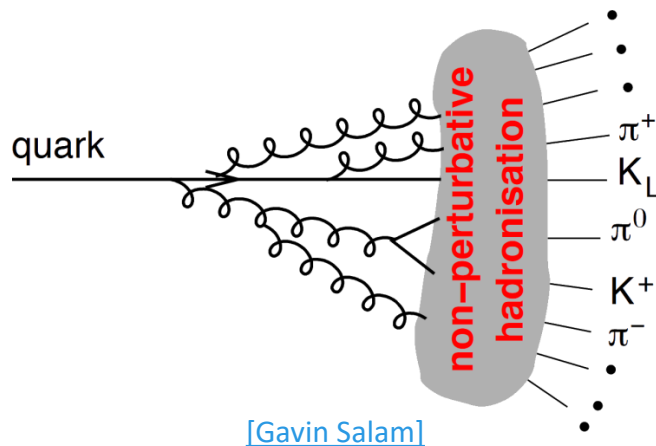


# Jet Production and Detection in ATLAS

**ATLAS:** multi-purpose **particle detector**

**Jet:** collimated **spray of hadrons** produced by the **hadronization of a quark or a gluon**

→ Produce **tracks** in the trackers and **energy deposits** in the calorimeters, that are **clustered together** to obtain the properties of the initial quark or gluon



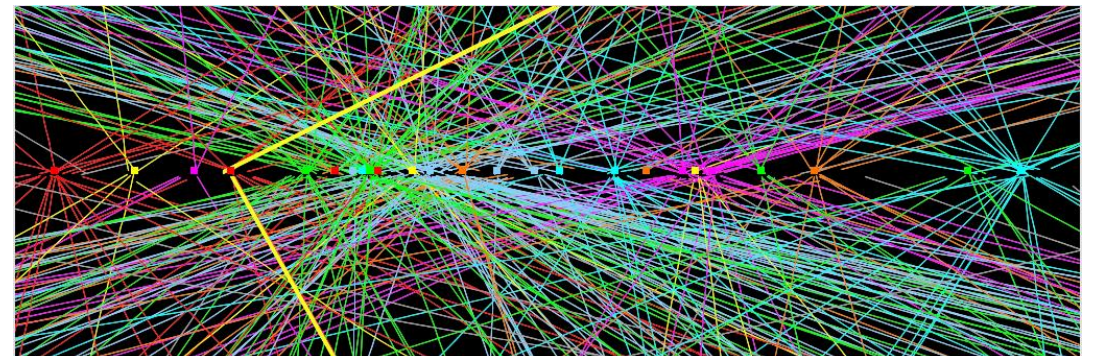
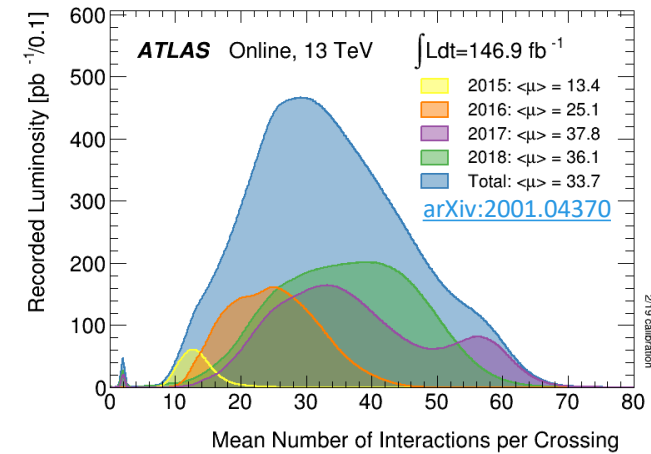
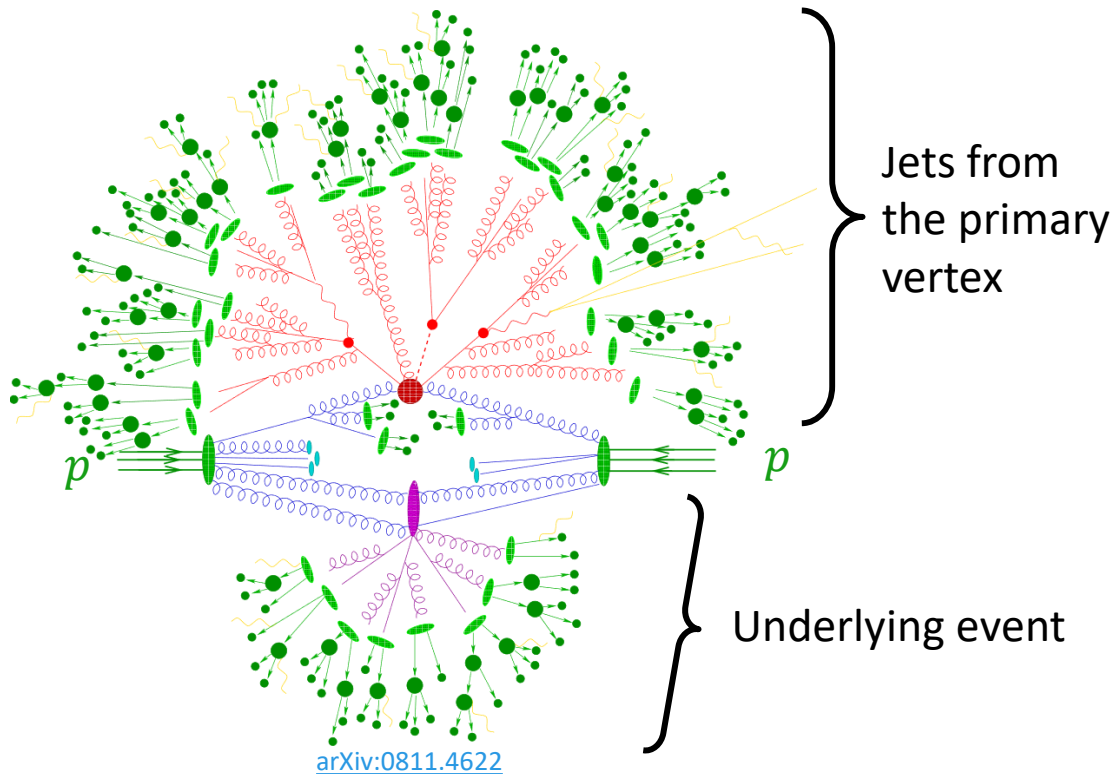


# Pileup

**Pileup:** all the effects of other interactions other than the hard scatter  
→ **Challenge** for the jet reconstruction and calibration

In-time pileup: underlying event, other collisions in the same bunch crossing

Out-of-time pileup: collisions in other bunch crossings



# Jet Reconstruction in ATLAS used during Run 2

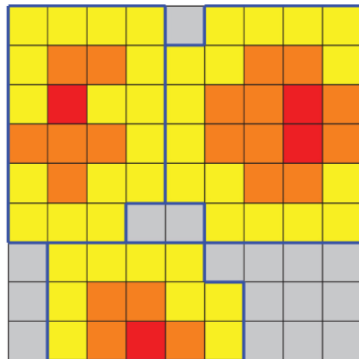
**Step 1:** Building particle-like clusters from the energy deposits and the tracks

## Topological clusters

[arXiv:1603.02934](https://arxiv.org/abs/1603.02934)

Connect group of calorimeter cells

- 1) Seed: cell with  $|E| > 4\sigma$
- 2) Growth: adjacent cells with  $|E| > 2\sigma$
- 3) Additional layer
- 4) Splitting algorithm (local maxima)



Boundary cells   Growth cells   Seed cells  
Empty cells   Topocluster

[Deepak Kar]

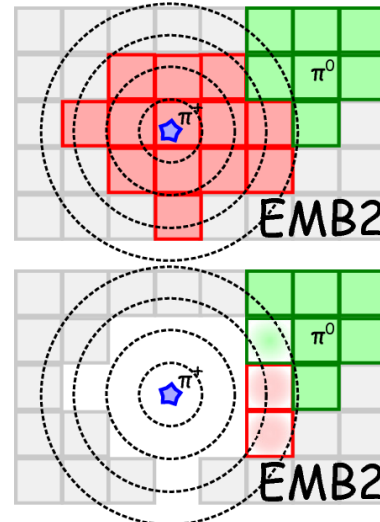
## Particle flow objects (PFOs)

[arXiv:1703.10485](https://arxiv.org/abs/1703.10485)

Combine track and cluster information

→ Better resolution at low  $p_T$ , pileup separation

- 1) Select good tracks
- 2) Subtract them from the topo-clusters



**Step 2:** Building jets from clusters/PFOs

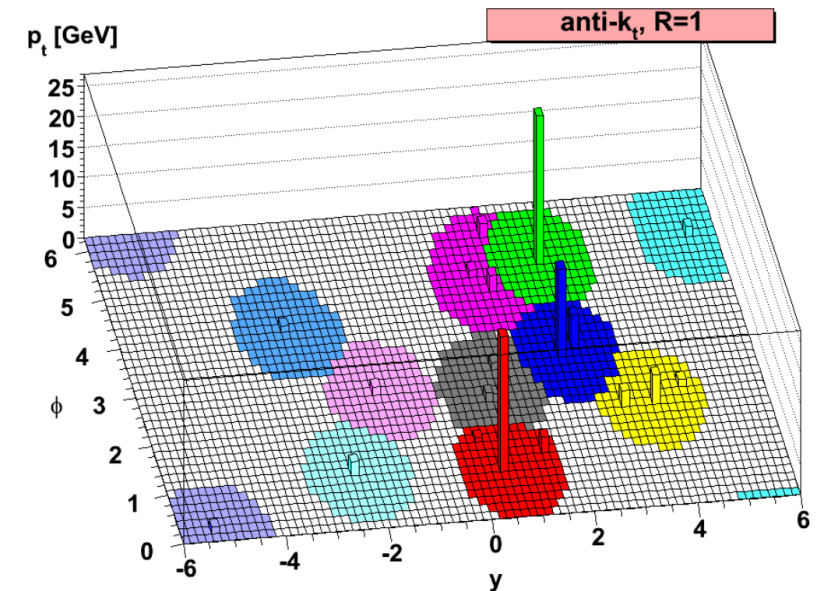
## Anti- $k_t$ algorithm

[arXiv:0802.1189](https://arxiv.org/abs/0802.1189)

Sequentially gather nearby constituents

Small radius jets: parameter  $R = 0.4$

Large radius jets: parameter  $R = 1.0$



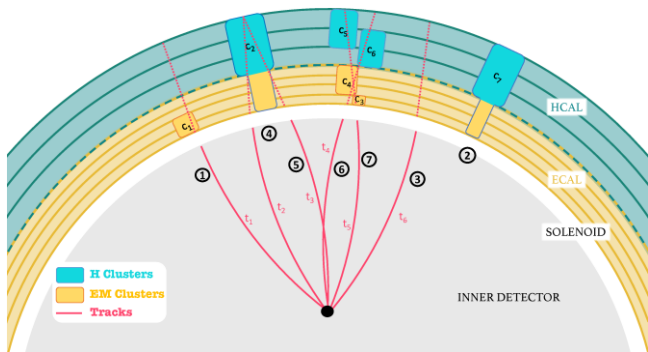
# Unified Flow Objects

## Track-CaloClusters (TCC)

[ATL-PHYS-PUB-2017-015]

Use **tracks** to **split up large clusters** based on the energy flow and their direction.

→ **Improvement of the mass resolution at high- $p_T$**



## Unified Flow Objects (UFOs)

arXiv:2009.04986

[ATL-PHYS-PUB-2022-038]

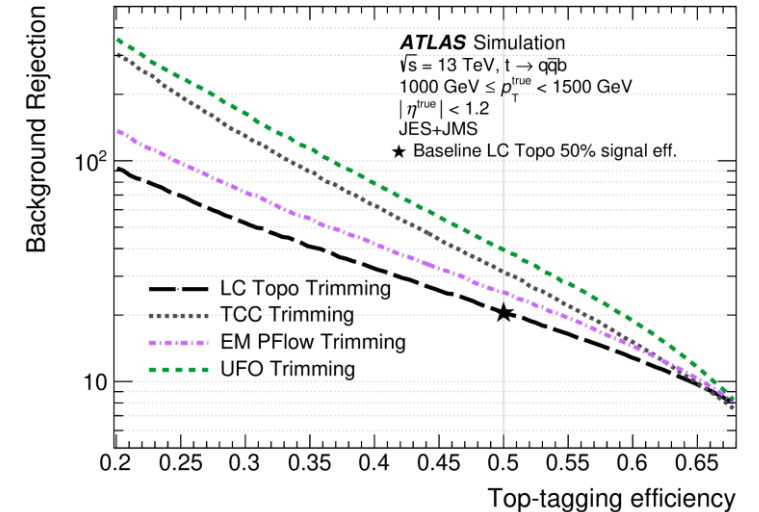
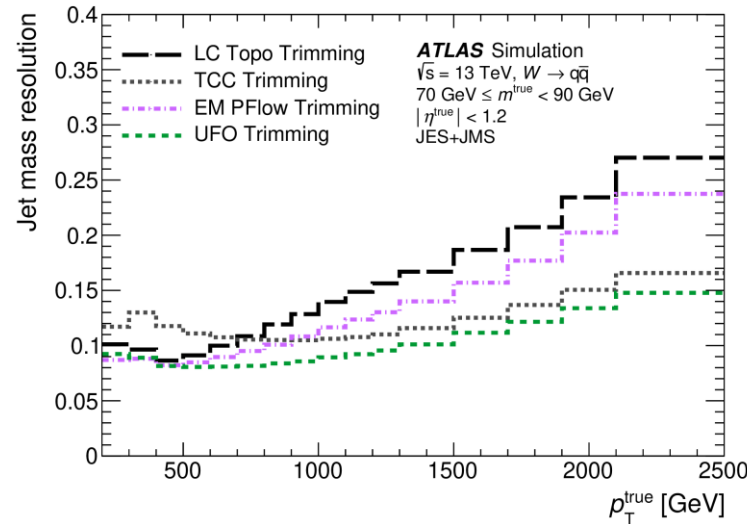
Apply TCC technique to split PFOs

→ Low  $p_T$ : good pileup subtraction from PFOs

→ High  $p_T$ : large clusters are split

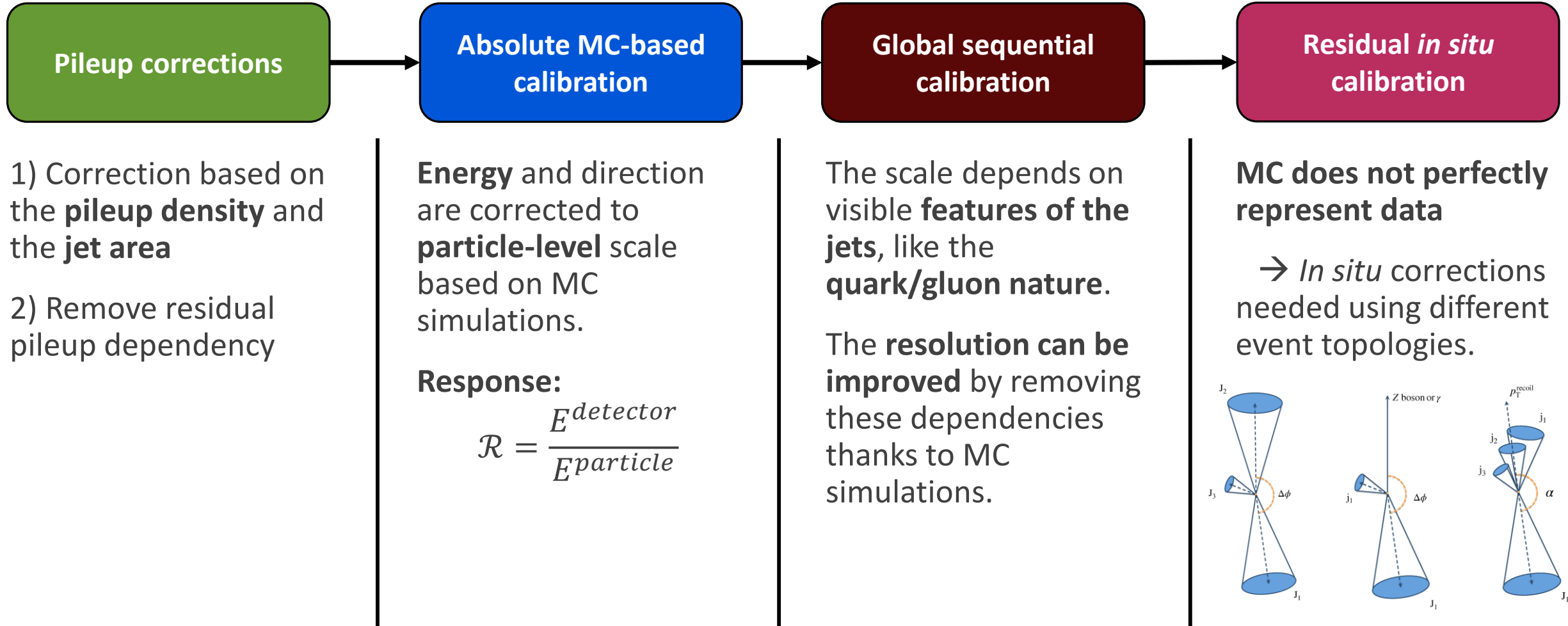
→ **Best mass resolution across  $p_T$**

→ **Best background rejection** for a simple top-tagger at both low and high  $p_T$



Results shown here for large radius jets ( $R = 0.1$ ); results for small radius jets in [backup](#).

# Small- $R$ Jet Energy Scale Calibration used in ATLAS during Run 2



[Backup: small- \$R\$  JES calibration more in depth](#)



# The Uncertainties on the Jet Energy Scale

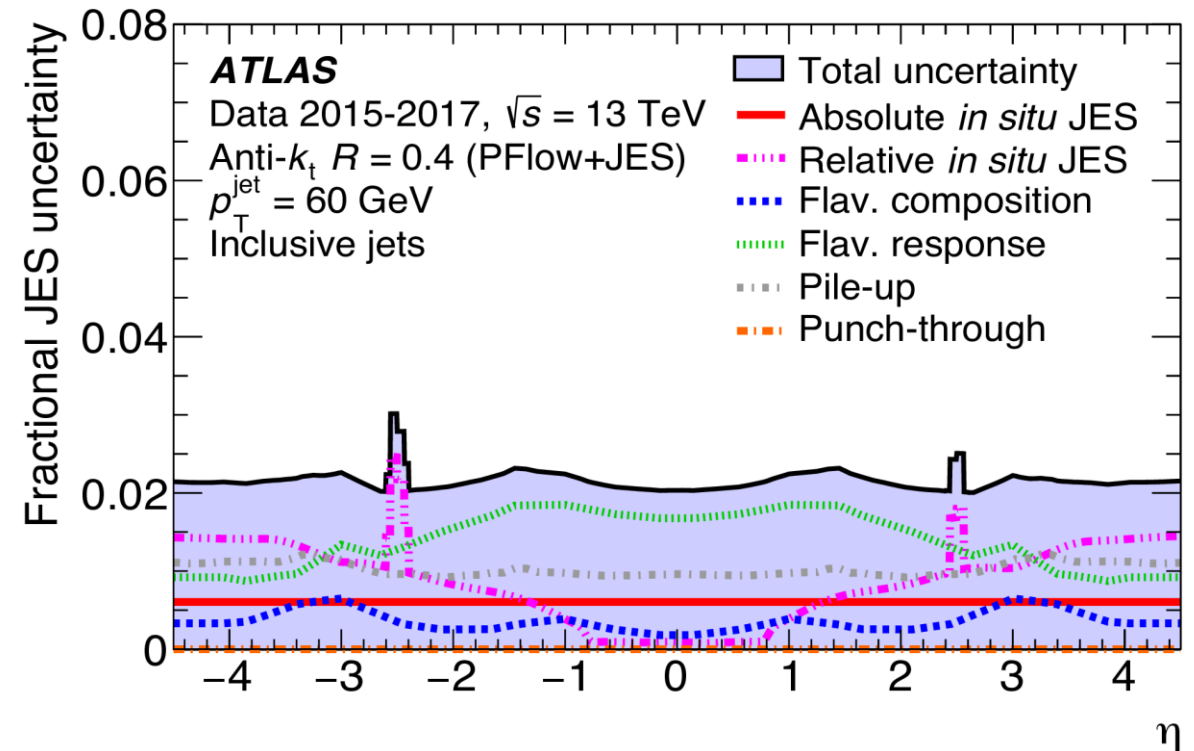
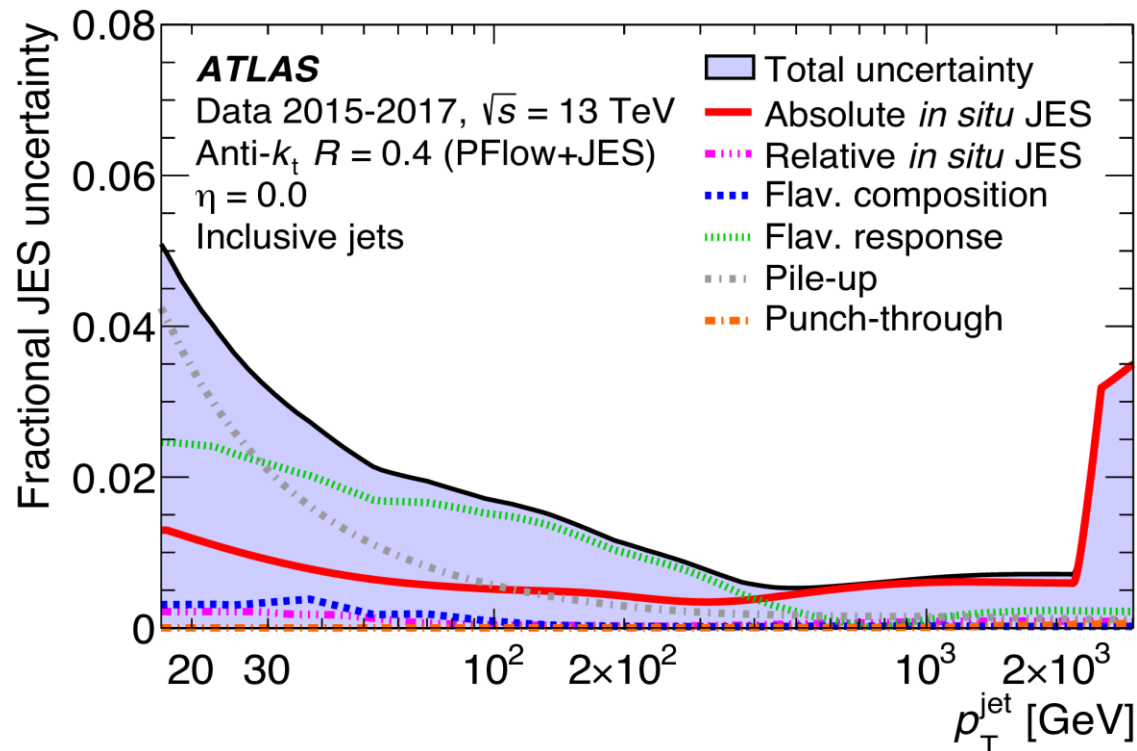
Improvements of some dominant uncertainties:

Flavour uncertainties ([slides 15-17](#))

$\eta$ -intercalibration ([slide 12](#))

$E/p$  (high- $p_T$ ) ([slide 13](#))

Pileup (backup [1](#), [2](#))





# Global Neural Network Calibration

The Global Sequential Calibration (**GSC**) **sequentially** corrects for the response dependency on six variable so does not exploit correlations.

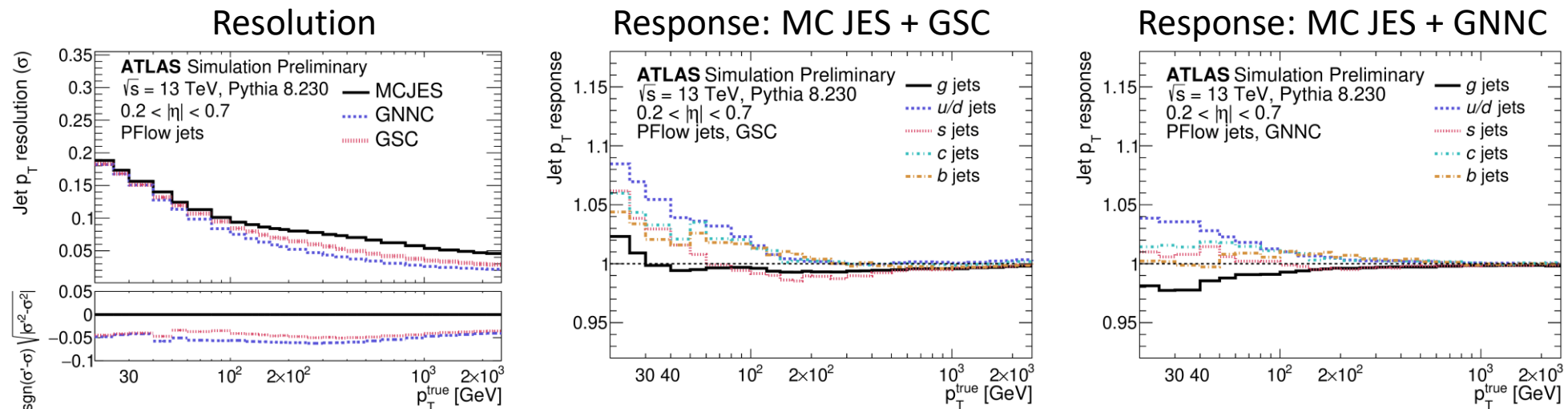
The Global Neural Network Calibration (**GNNC**) uses a **Deep Neural Network (DNN)** trained to predict the  $p_T$  response. **It can use more correlated variables.** [Architecture](#) and [inputs](#) in backup.

→ The Jet Energy Resolution (JER) is improved by 15 – 25 % on average compared to the GSC.

→ The responses of quark-initiated jets is closer to unity → Reduction of the flavour uncertainties.

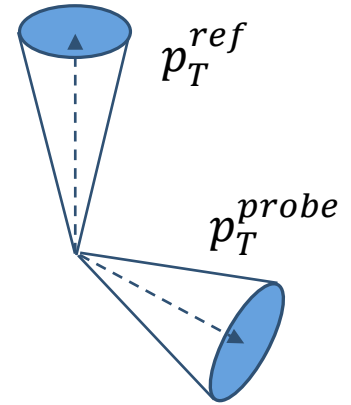
(→ see [slide 15](#))

The *in situ* studies allow to validate the improvements in the calibration chain (see [backup](#)).



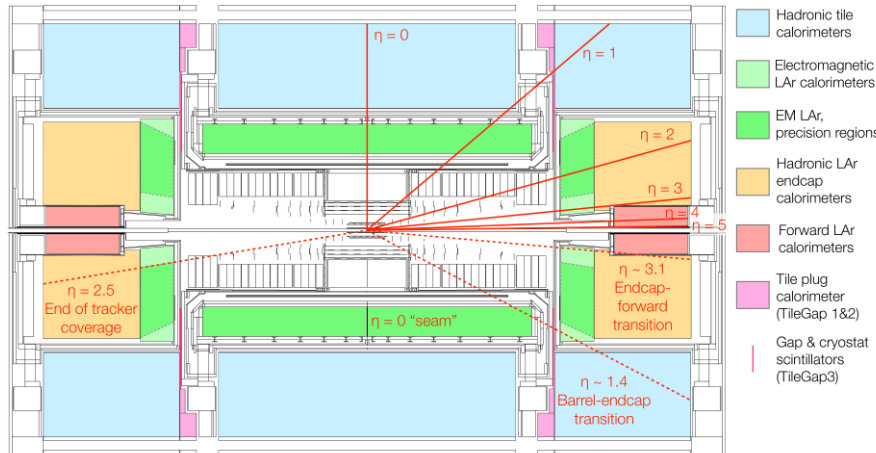
# $\eta$ -intercalibration Uncertainty Reduction

**In situ  $\eta$ -intercalibration:** make the calibration homogeneous across the whole  $\eta$  range using dijet events and transverse momentum conservation:  $c = p_T^{ref} / p_T^{probe} \approx 1$ .

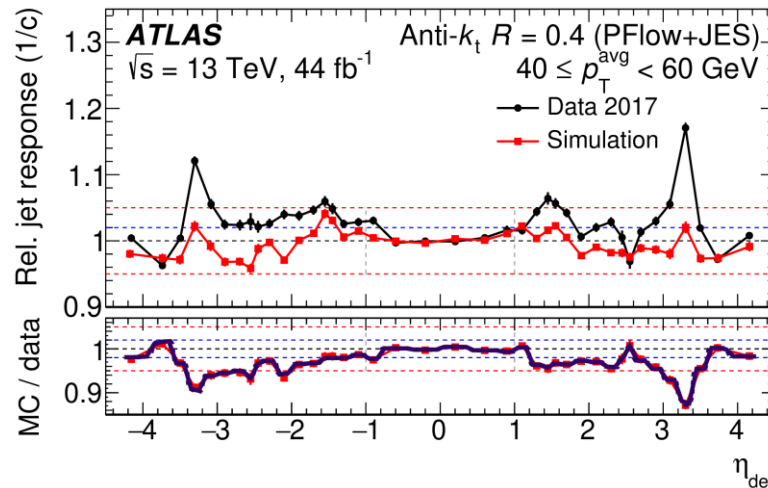


## Modelling differences affect:

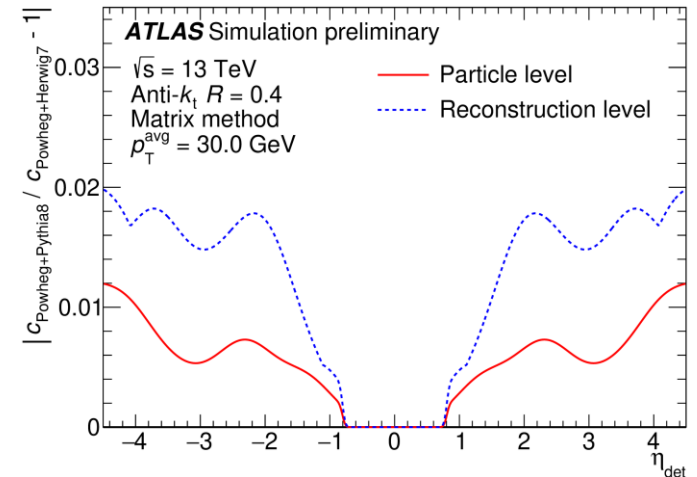
- the dijet balance (extra radiations like a third jet, out-of-cone radiations)
- the detector response (through the jet composition and substructure)
  - Possible **double-counting of detector effects with the flavour uncertainty.**
  - Solution: separating physics effects from detector effects
  - **Factor 2 reduction** of the modelling uncertainty below 40 GeV, which was dominant



Calibration



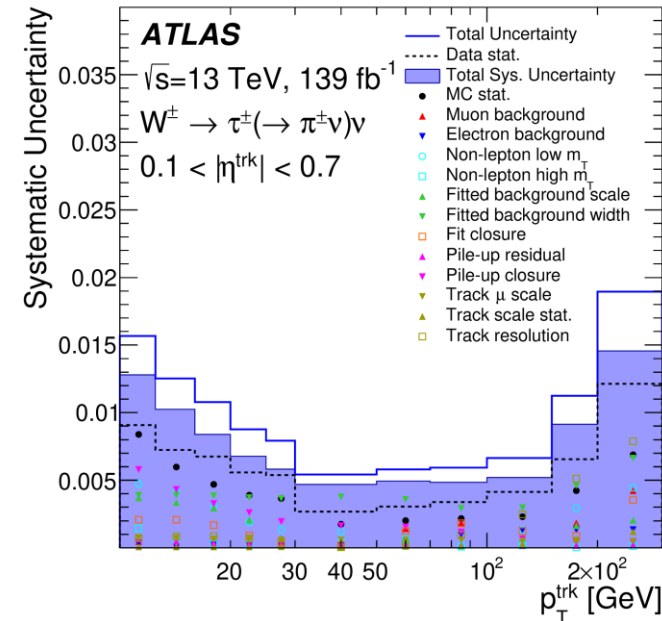
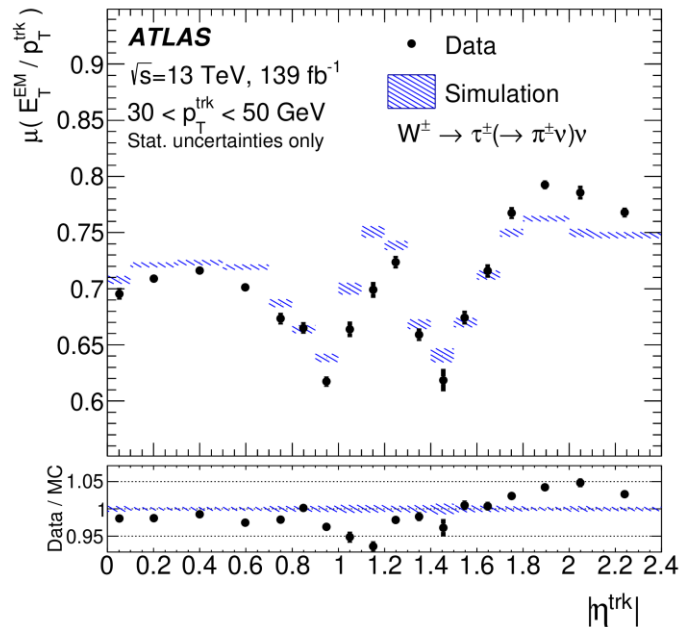
Modelling uncertainty



# $E/p$ Calibration Using $W^\pm \rightarrow \tau^\pm (\rightarrow \pi^\pm \nu_\tau) \nu_\tau$ Events

$W^\pm \rightarrow \tau^\pm (\rightarrow \pi^\pm \nu_\tau) \nu_\tau$  events provide **highly-energetic isolated charged pions**

Gaussian fit of the  $E^{\text{calorimeter}}/p_T^{\text{tracker}}$  distribution in data and MC



→ Calorimeter response obtained in a very wide range ( $10 < p_T < 2000$  GeV and  $|\eta| < 2.4$ )

→ Excellent precision → High  $p_T$  uncertainties improvement

→ Improvement over the combined test-beam data previously used

[More  \$E/p\$  results](#)



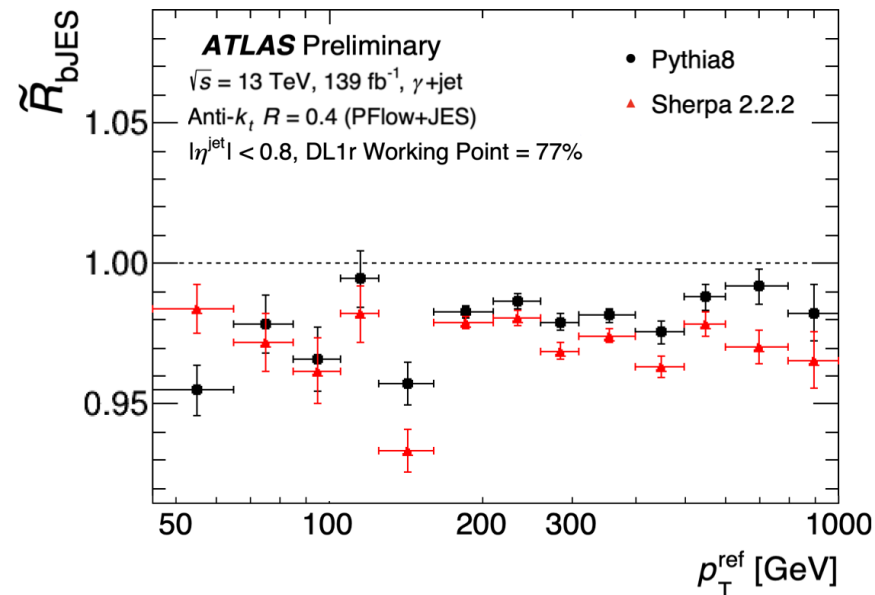
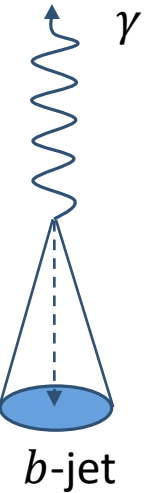
# $b$ Quark Jet Energy Scale in $\gamma$ +jet Balance

**$\gamma$ +jet balance:** exploit the transverse momentum balance between a jet and a reference photon.

The MC-to-data response ratio is obtained for two selections: inclusive, and  **$b$ -tagged jets**.

$$\tilde{\mathcal{R}}_{bJES} = \frac{\mathcal{R}_{b\text{-tagged}}^{MC} / \mathcal{R}_{b\text{-tagged}}^{data}}{\mathcal{R}_{inclusive}^{MC} / \mathcal{R}_{inclusive}^{data}}$$

The energy scale of  **$b$ -tagged jets with respect to that of inclusive jets** is determined in with a precision of about **1.5 to 2 %** on a broad phase-space range.



→ Will improve measurements of:

- Top mass
- Bottom Yukawa ( $VH, H \rightarrow b\bar{b}$ )

[b-JES for different b-tagger working points in backup](#)

# The Flavour Uncertainty

Different MC generators, different hadronization models

→ Different fragmentation pattern and hadron content

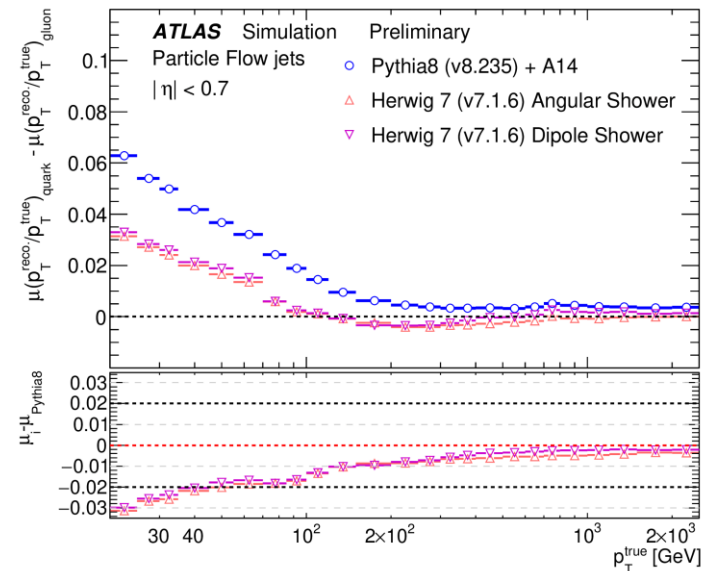
→ Different detector responses

→ Flavour uncertainty

Origin: non-compensating nature of the calorimeters.

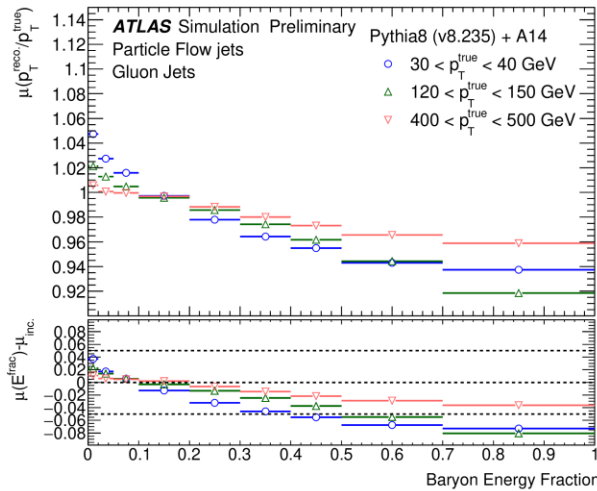
Response of  $\pi^0$  and  $\pi^\pm$  are very different. Response of pions, kaons, baryons are different too.

→ Important response difference observed between quark and gluon jets



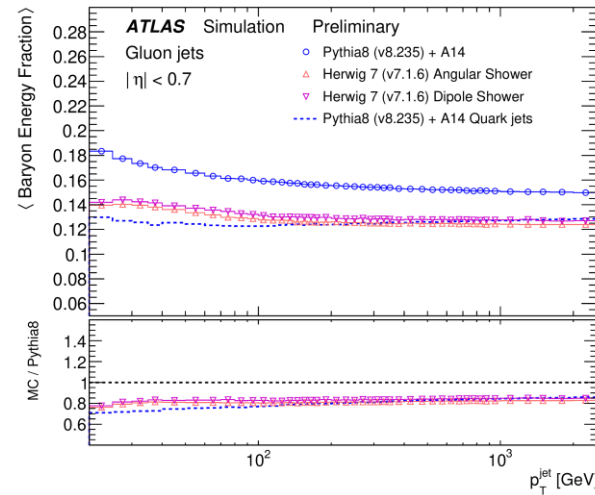
# Response of Gluon Jets vs. Baryon Energy Fraction

Dependency of the response on the **baryon energy fraction**

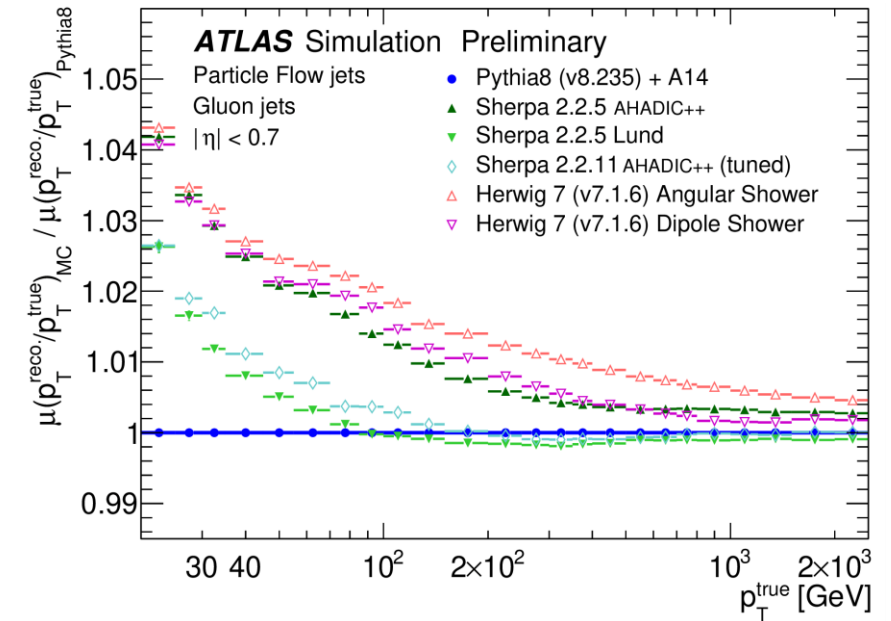


+ Similar observations for kaons, see [backup](#)

**Different baryon energy fraction between Lund string-based and cluster-based hadronization models**



**Response difference between the two types of hadronization models**



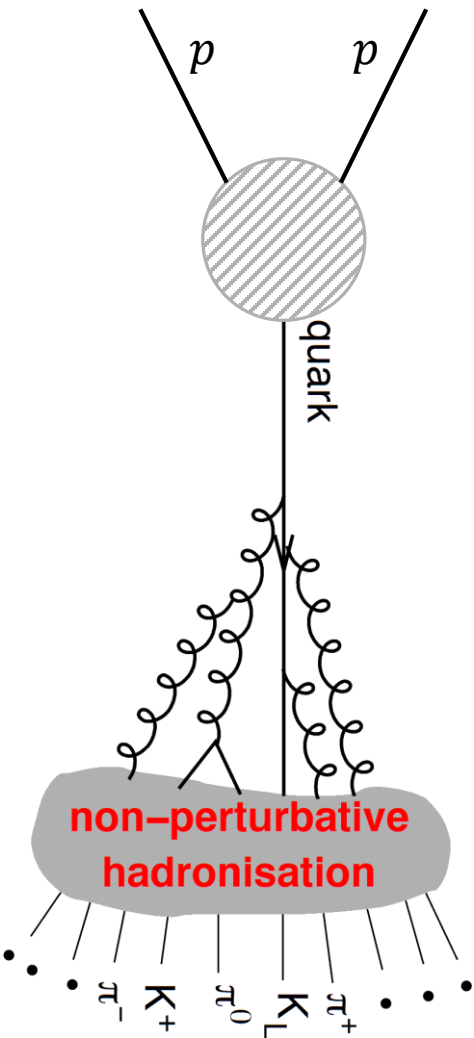
**Fragmentation pattern + hadron content → need to be tuned to experimental measurements**

Reweighting the events based on the baryon and kaon energy fractions reduces the differences ([backup](#))

**Reduction in the dependence on the generator configuration would result in a significant improvement of the flavour uncertainties.**



# Flavour Uncertainty Decomposition



## Matrix element generation

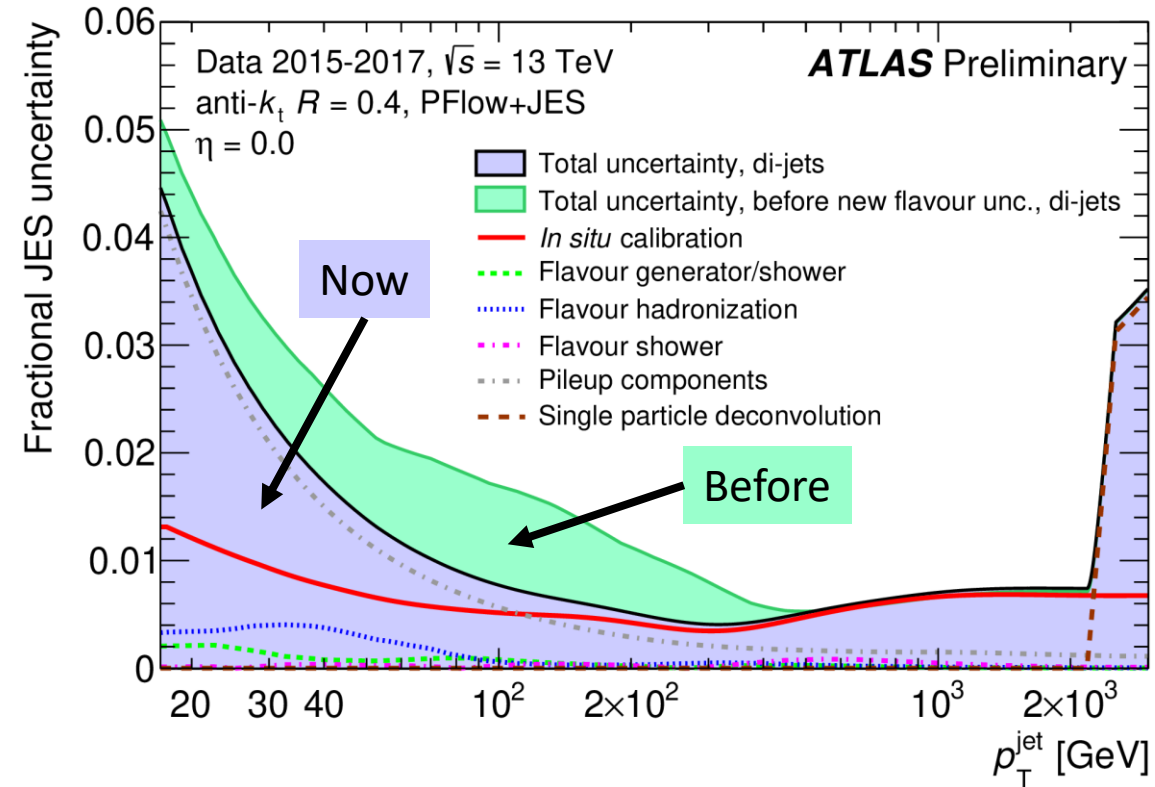
→ Difference of responses between Pythia8 and Sherpa + Lund string hadronization

## Shower model

→ Difference of responses between Herwig7 + angular-ordered shower and Herwig7 + dipole shower

## Hadronization model

→ Difference of responses between Sherpa + cluster-based hadronization and Sherpa + Lund string hadronization



→ Previous treatment: 2 components: sample composition + response difference of gluon-initiated jets between Pythia8 and Herwig7

→ New treatment: 3 components

→ **Improvement of the overall flavour uncertainty**

# Conclusion

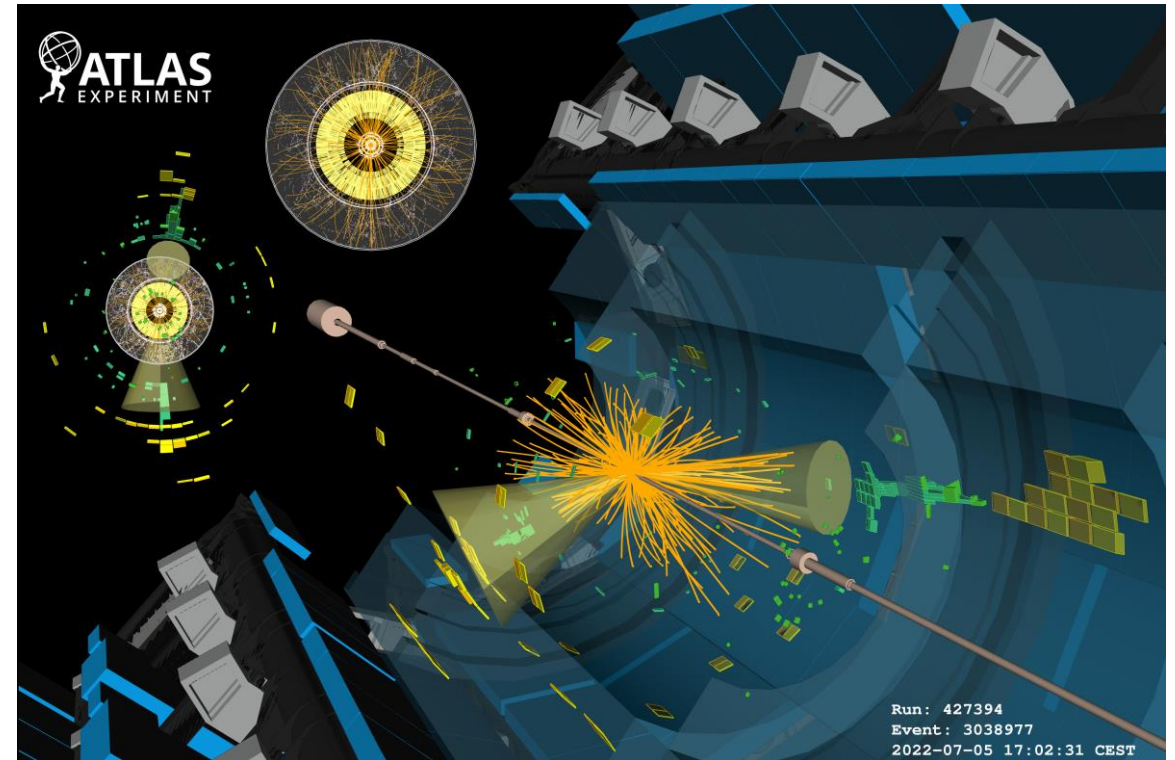
**Hadronic objects reconstruction and calibration are important for precision measurements and BSM exploration at the LHC (and beyond)**

**Lots of improvements** at every step of the definition and calibration of jets, thanks to the exploration of new techniques

→ Also see the use of ML/AI techniques for hadronic object performance (see Reina Camacho's talk)

**Run 3 just started:** great opportunity to exploit these developments and continue refining our strategies

→ Lot of work ongoing in that direction, stay tuned!



Run 3 dijet event

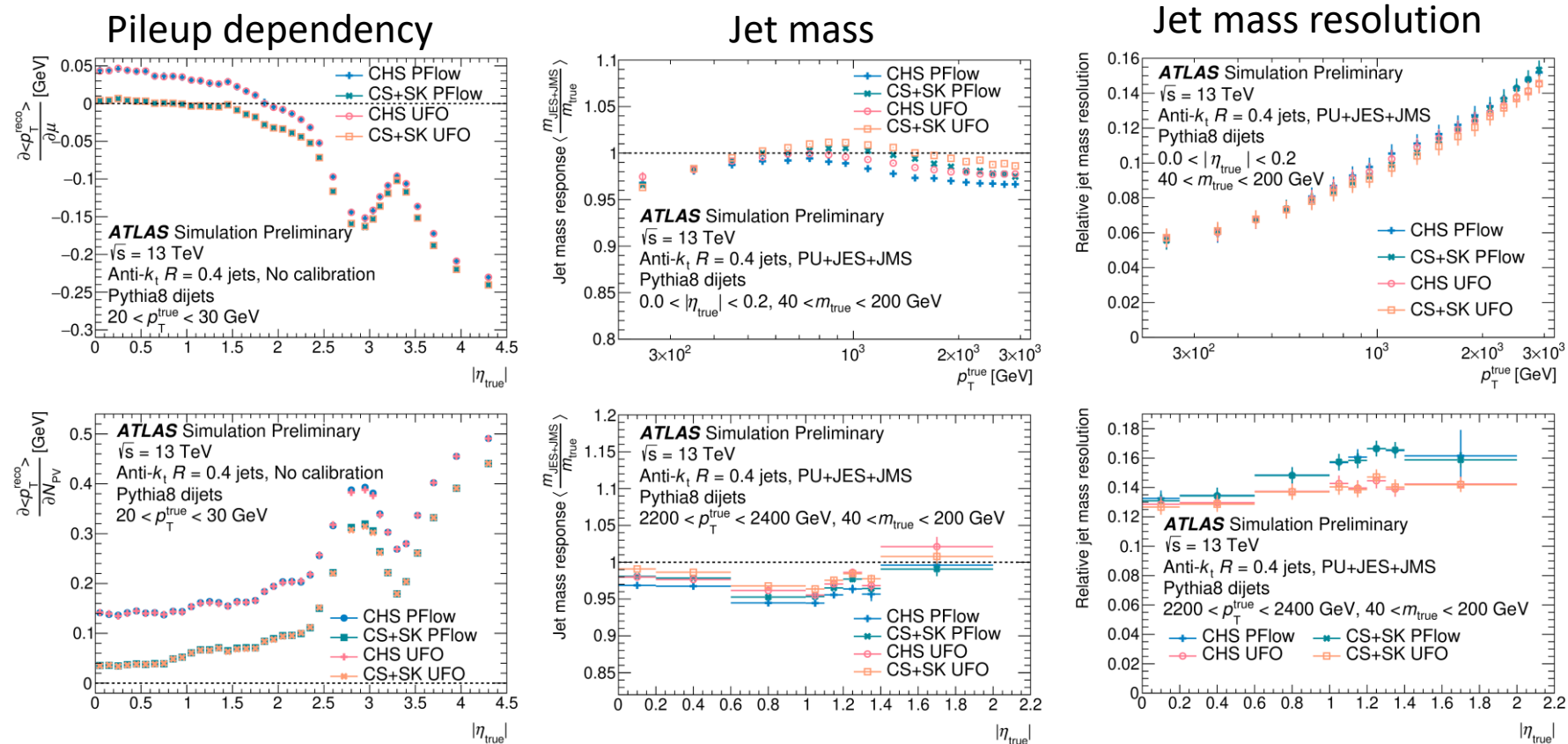
# Backup



# UFOs and CS+SK for small- $R$ jets

CS+SK reduces the pileup dependency (see next slide).

CS+SK UFO → **Better calibration of the jet mass and better mass resolution.**  
 → Consistent with PFlow jets on other observables.



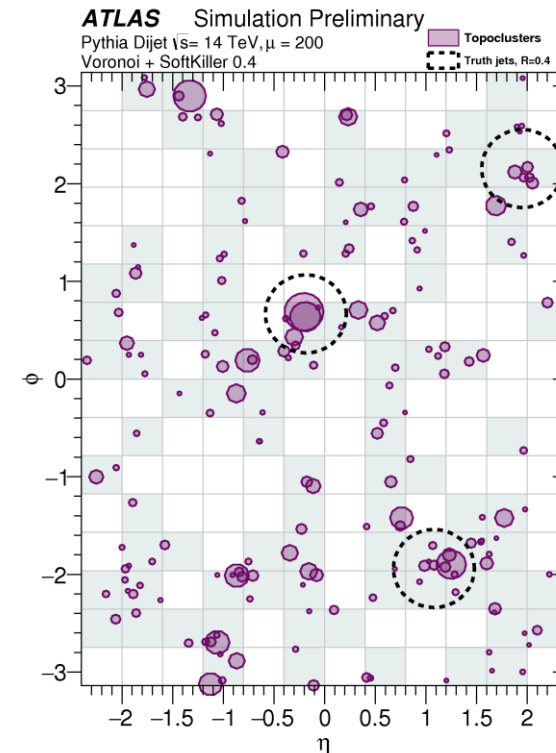
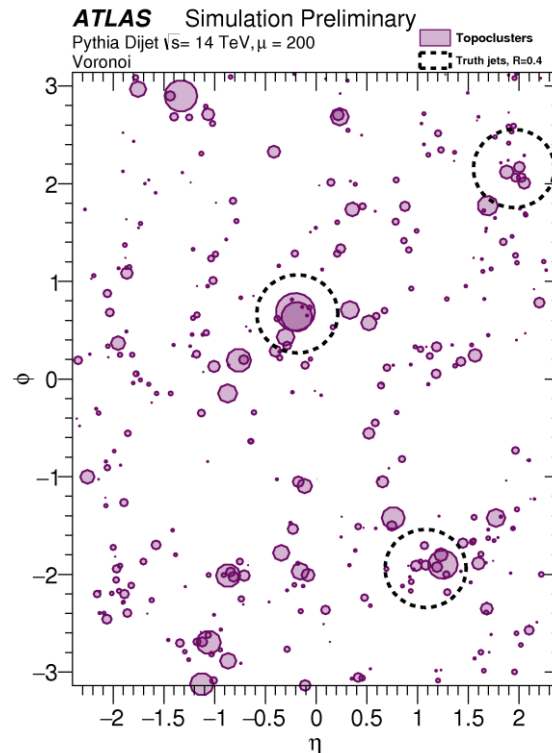
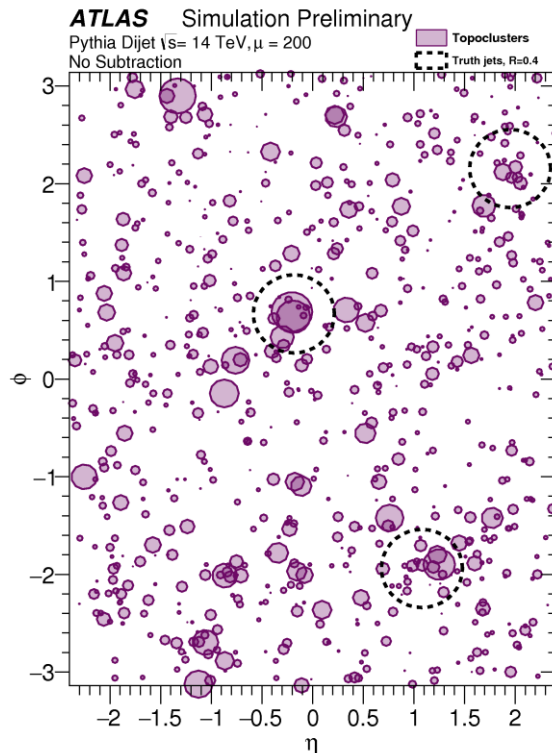
[Back to UFO for large- \$R\$  jets.](#)

# CS+SK

Some pileup can be removed prior to jet reconstruction

→ Constituent subtraction (CS): assign an area to each cluster in  $(\eta, \phi)$  (region where points are closer to that cluster than any other cluster), and subtract the expected pileup for that area.

→ Soft killer (SK): divide the event into a grid and remove the squares below a threshold.



# Small-R JES Calibration more in depth

## Pileup corrections

## Absolute MC-based calibration

## Global sequential calibration

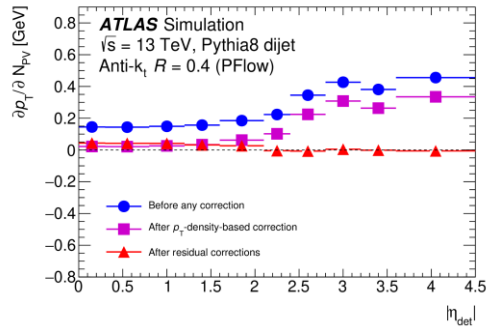
## Residual *in situ* calibration

1) **Area-based correction** with pile-up density  $\rho$  and jet area  $A$ .

2) **Local MC-based correction.** Characterization:

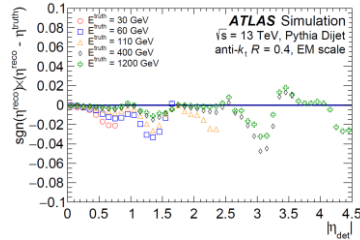
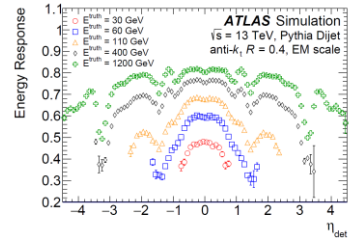
- In-time pileup:  $N_{PV}$
- Out-of-time pileup:  $\mu$

$$p_T^{corr} = p_T^{reco} - \rho A - \alpha(N_{PV} - 1) - \beta\mu$$



1) **Energy** is calibrated to the true jet energy from MC using a smooth multiplicative function in bins of  $\eta$ .

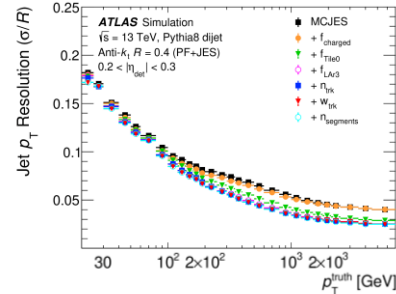
2) **Direction  $\eta$**  receives an additive correction.



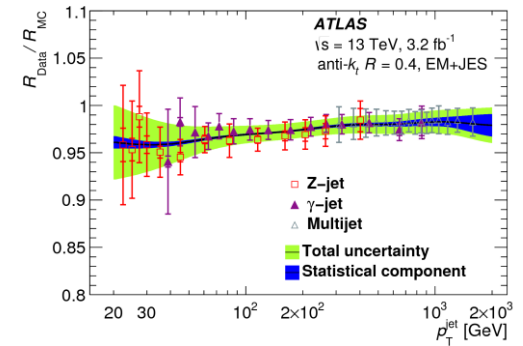
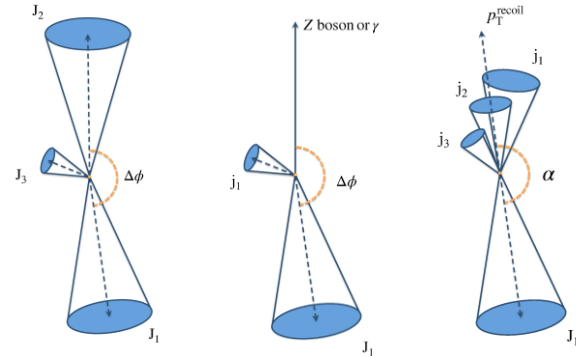
The scale depends on visible **features of the jets**, like the **quark/gluon nature** or the energy in dead material.

The **resolution can be improved** by removing these dependencies thanks to MC simulations.

This is done sequentially for 6 variables.



MC does not perfectly represent data  $\rightarrow$  *In situ* corrections needed using different event topologies.





# Improved Pileup Energy Density Determination

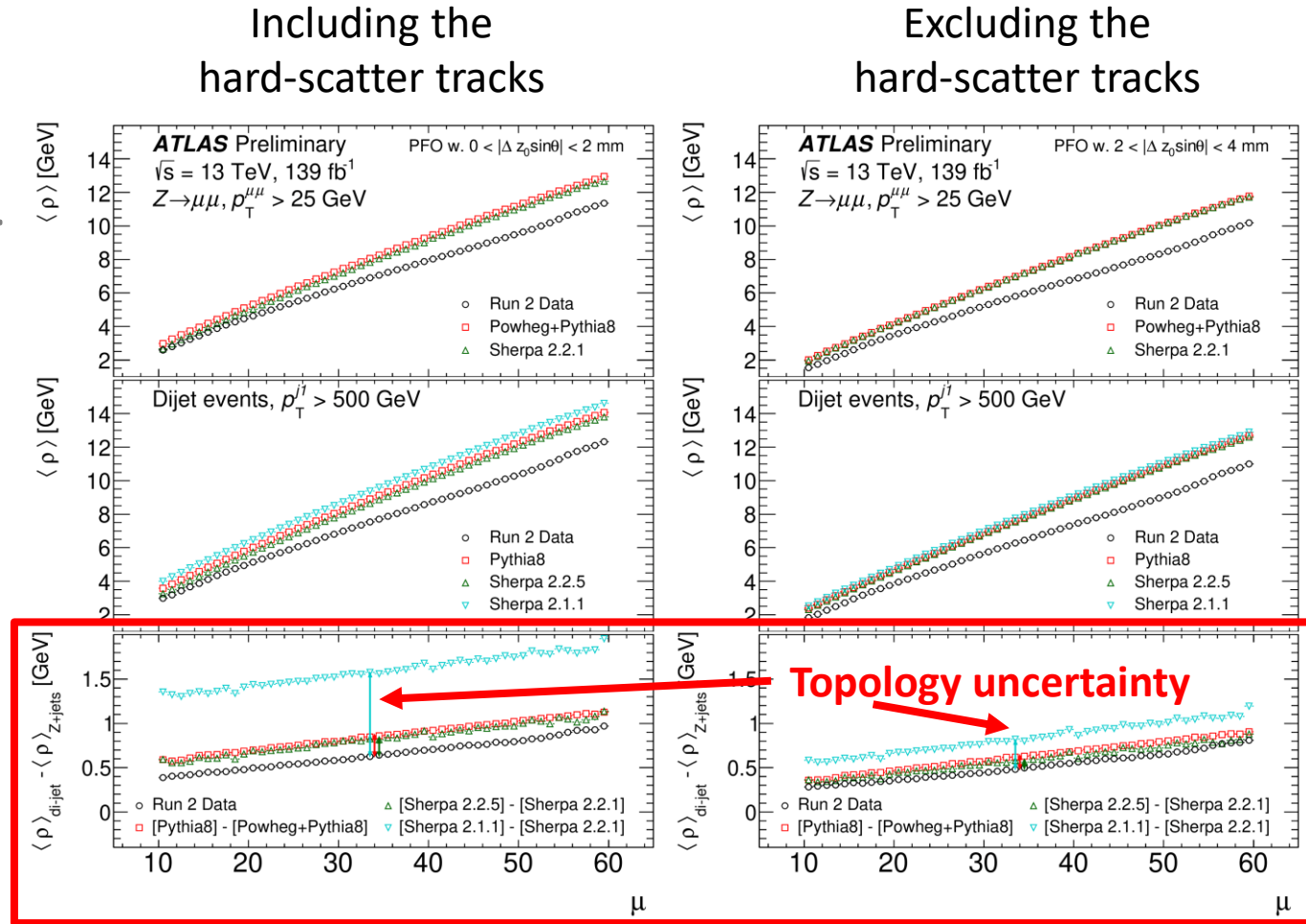
Pile-up energy density  $\langle \rho \rangle$  determination:

$$\langle \rho \rangle = \text{median}_{i \in \{\text{jets}\}} \left( \frac{p_{T,i}}{A_i} \right)$$

for two different selections:  $Z \rightarrow \mu\mu$  and dijet events.

- Previous determination was including the hard-scatter tracks
  - **Reduction in the dependency on hard scattering topologies**
  - Improvement on topology uncertainties by a factor of 3
- Updated Sherpa Multi-Parton Interaction (MPI) results in a factor of 4 improvement
- **Total improvement of nearly a factor 7 of the topology uncertainty**

[Back to the JES uncertainties](#)



# Improved Pileup Residual Correction

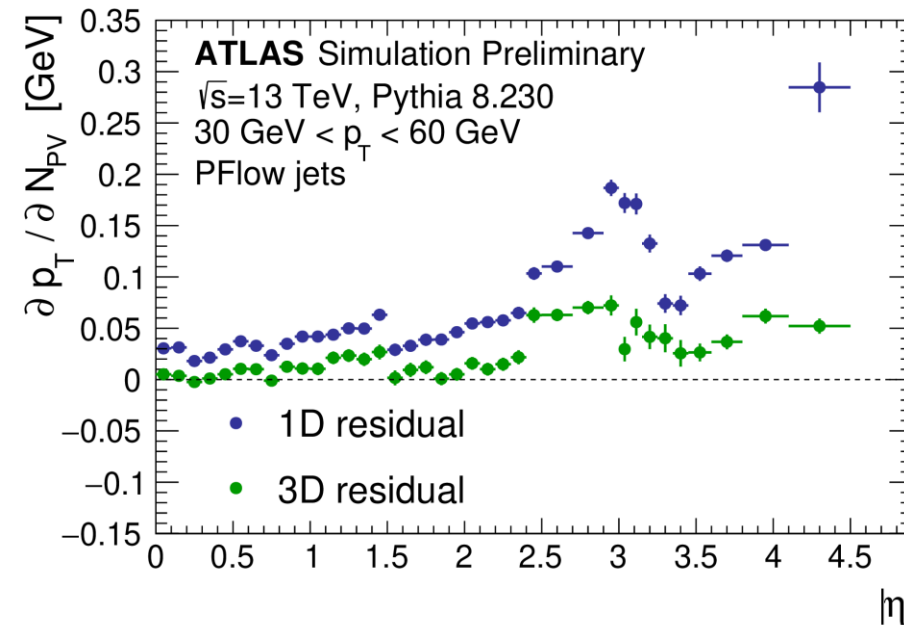
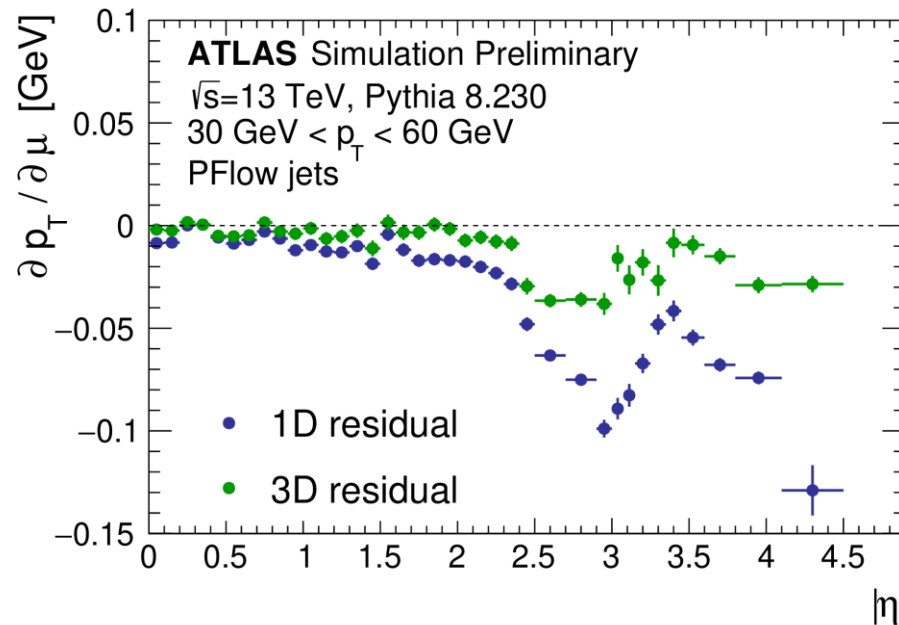
**1D** residual pileup correction:  $p_T^{corrected} = p_T - \alpha(N_{PV} - 1) - \beta\mu$

[Back to the JES uncertainties](#)

**3D** residual correction:  $p_T^{corrected} = p_T - \Delta p_T(N_{PV}, \mu, \eta, p_T)$

The 3D residual correction **takes into account correlations between  $N_{PV}$ ,  $\mu$  and jet properties.**

→ **Reduction of the pileup dependency above 30 GeV**



# GNNC architecture

---

3 hidden layers with swish activation functions ([arXiv:1710.05941](#)), each with 100 nodes, and a single-node output layer with linear activation.

Leaky Gaussian kernel loss function ([arXiv:1910.03773](#)), where the target is the jet  $p_T$  response.

[Back to the GNNC](#)

# GNNC inputs

[Back to the GNNC](#)

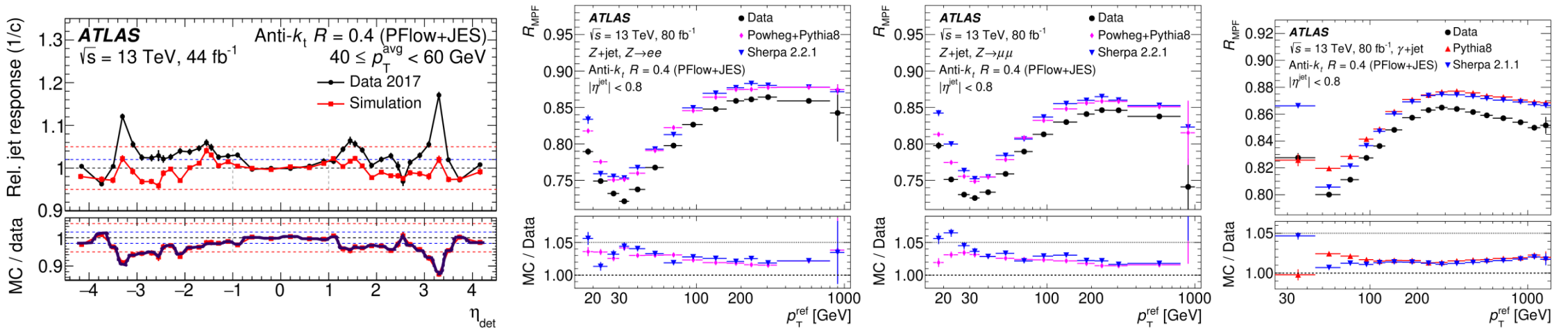
Calorimeter	$f_{\text{LAR},0-3}$	The fraction of energy measured in the 0th-3rd layer of the EM Lar calorimeter
	$f_{\text{TILE},0-2}$	The fraction of energy measured in the 0th-2nd layer of the hadronic tile calorimeter
	$f_{\text{HEC},0-3}$	The fraction of energy measured in the 0th-3rd layer of the hadronic end cap calorimeter
	$f_{\text{FCAL},0-2}$	The fraction of energy measured in the 0th-3rd layer of the forward calorimeter
	$N_{90\%}$	The minimum number of clusters containing 90 % of the jet energy
Jet kinematics	$p_T^{\text{JES}}$	The jet $p_T$ after the MC JES calibration
	$\eta_{\text{det}}$	The detector $\eta$
Tracking	$w_{\text{track}}$	The average $p_T$ -weighted transverse distance in the $(\eta, \phi)$ plane between the jet axis and all tracks of $p_T > 1$ GeV ghost-associated with the jet
	$N_{\text{track}}$	The number of tracks with $p_T > 1$ GeV ghost-associated with the jet
	$f_{\text{charged}}$	The fraction of the jet $p_T$ measured from ghost-associated tracks
Muon segments	$N_{\text{segments}}$	The number of muon track segments ghost-associated with the jet
Pileup	$\mu$	The average number of interactions per bunch crossing
	$N_{\text{pV}}$	The number of reconstructed primary vertices

# Validation of the MC calibration steps with the *In Situ* Techniques

Improvements in the MC calibration steps are validated thanks to the *in situ* calibration techniques.

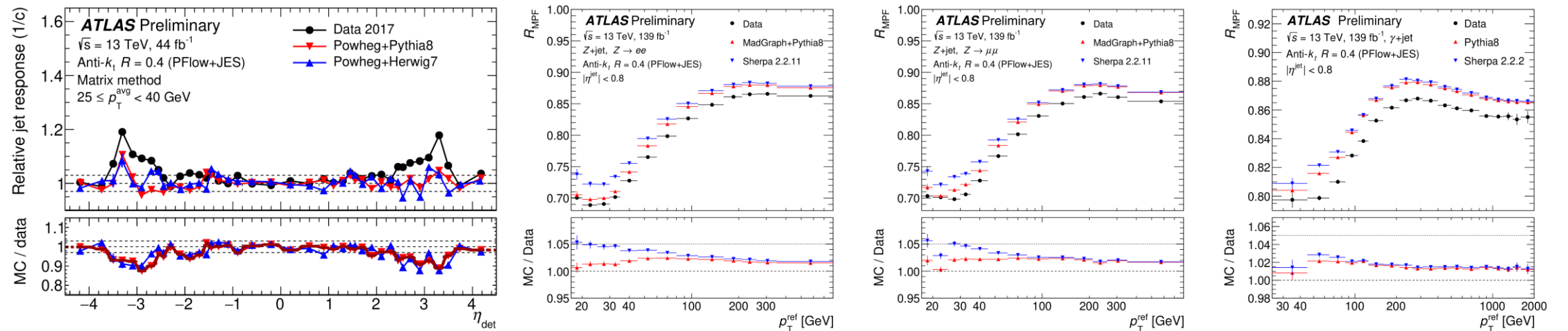
Previous *in situ* study

[arXiv:2007.02645](https://arxiv.org/abs/2007.02645)



New *in situ* study

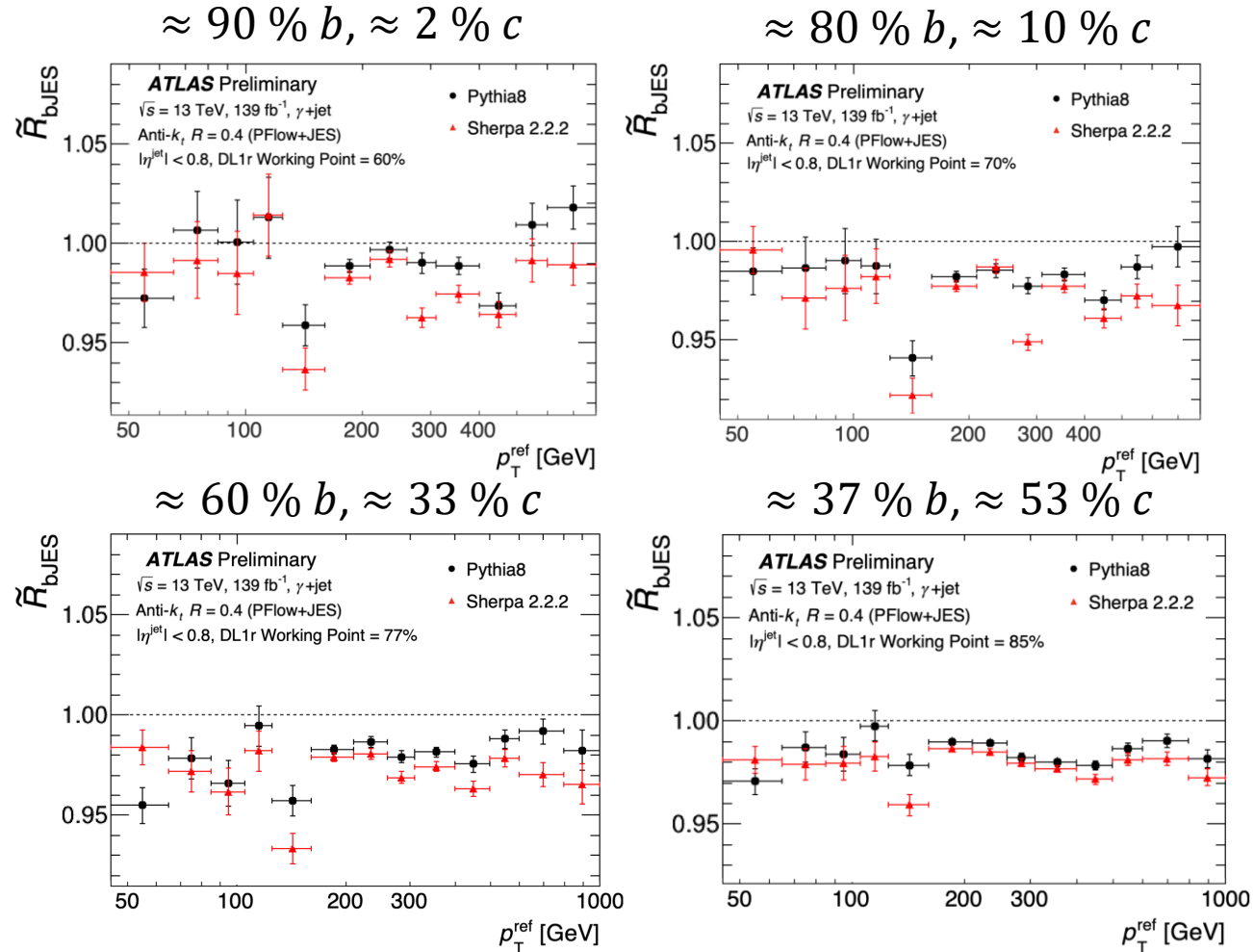
[JETM-2022-008](https://arxiv.org/abs/2022.008)





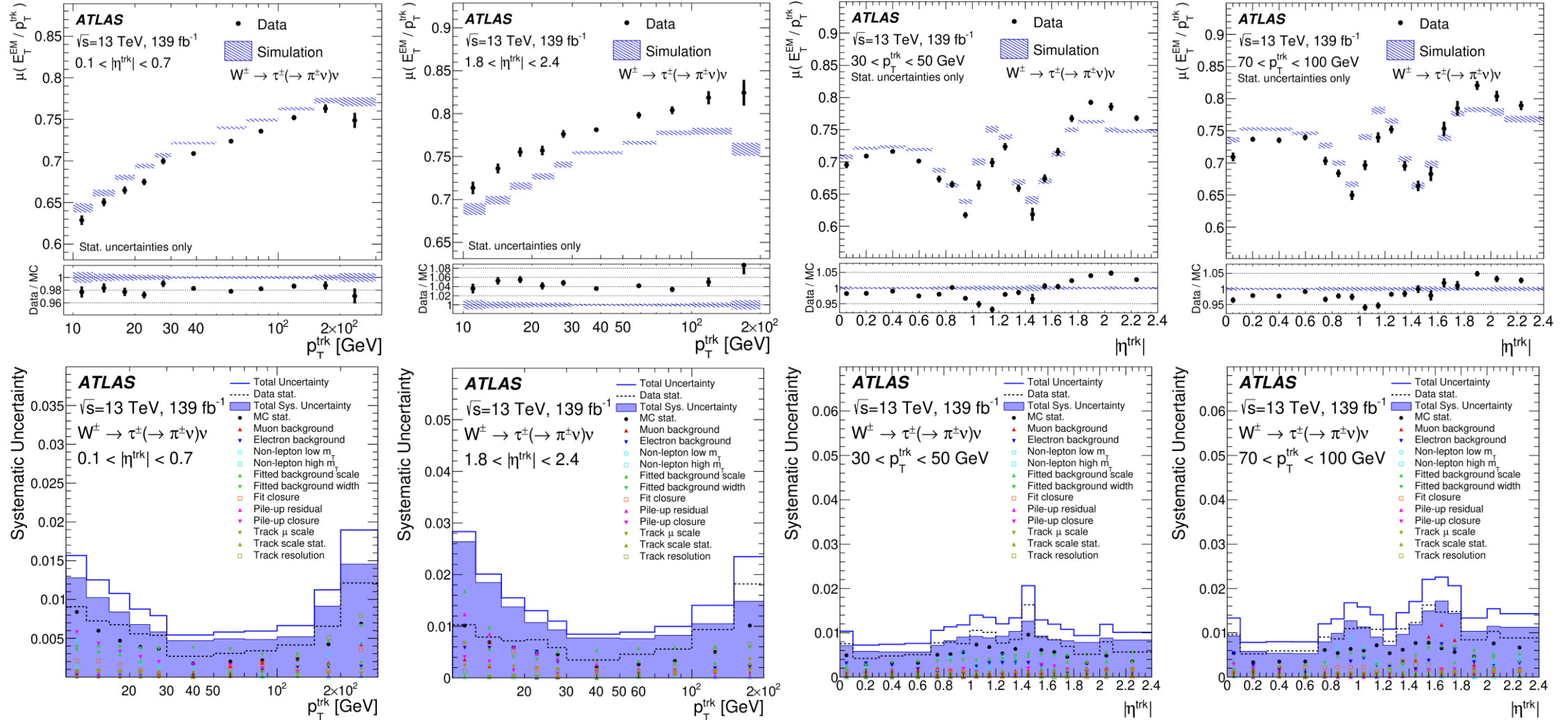
# $b$ Quark Jet Energy Scale for Different $b$ -tagging Working Points

Multiple  $b$ -tagger working point for different compositions of  $b$  quarks,  $c$  quarks, light quarks and gluons.



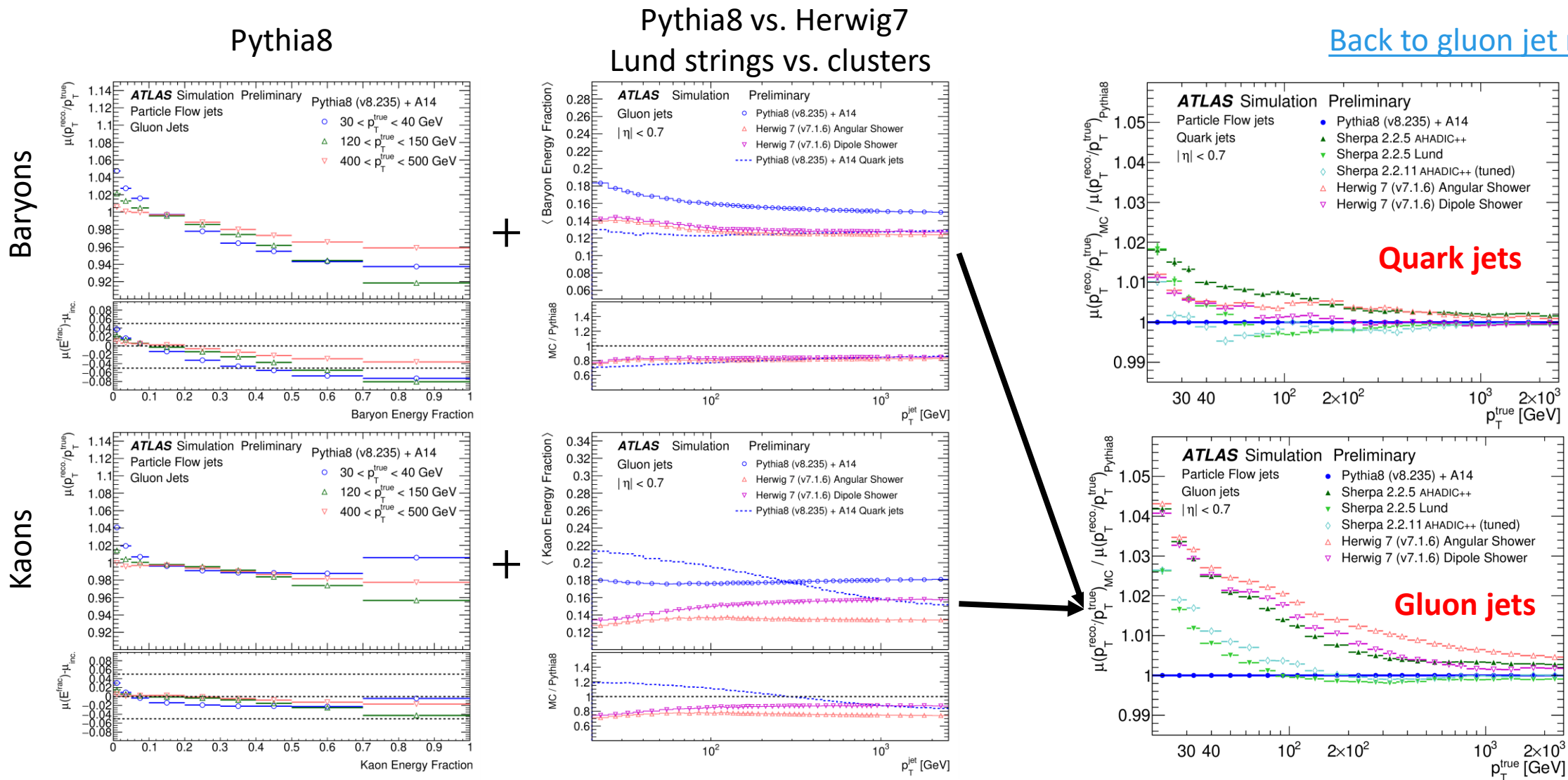
[Back to the  \$b\$ -JES](#)

# More $E/p$ results

[Back to  \$E/p\$](#) 


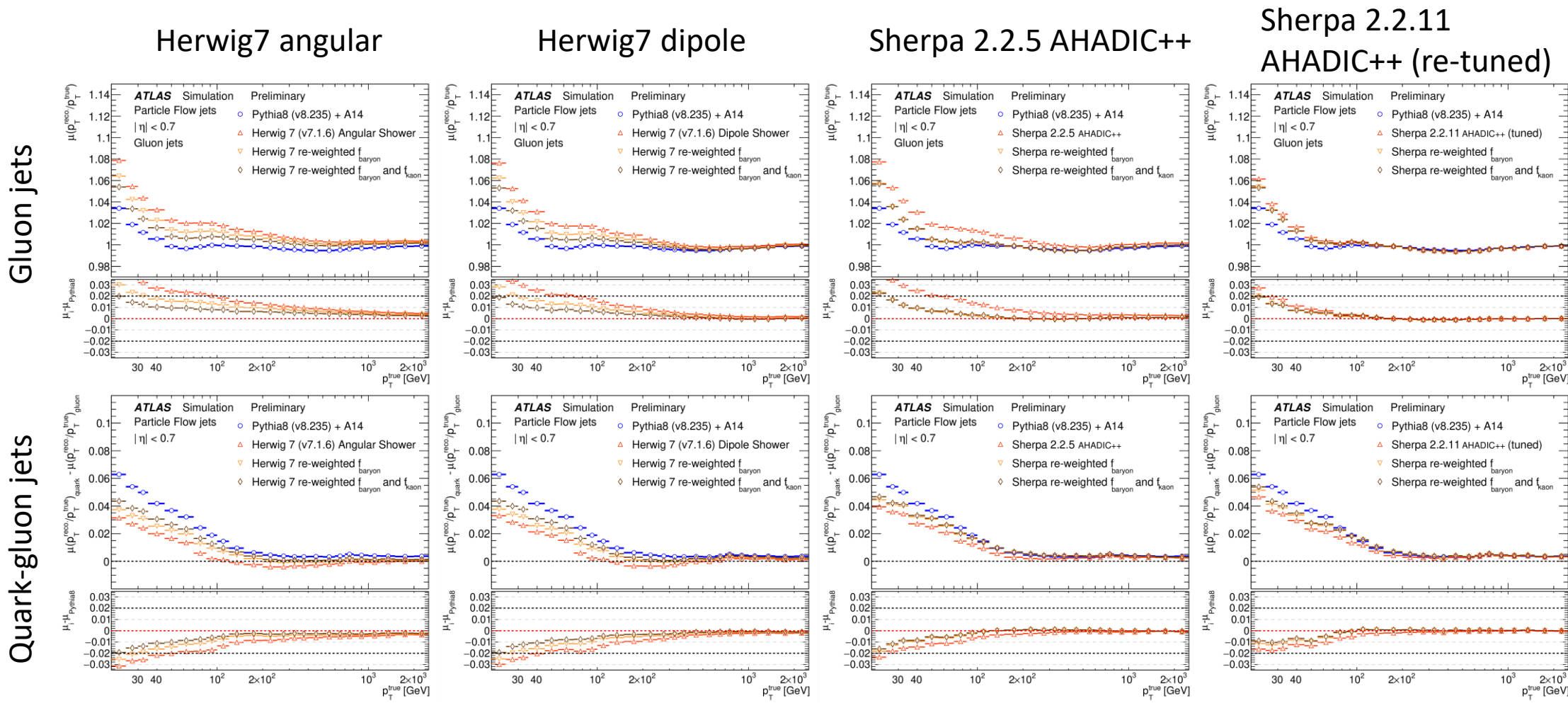
# Response of Gluon Jets vs. Baryon and Kaon Energy Fractions

[Back to gluon jet response](#)



# Response After Reweighting of Hadron Content

Reweighting the events based on the baryon and kaon energy fractions reduces the differences.



[Back to response of gluon jets](#)